J Comput Aided Mol Des (2011) 25:469–475
DOI 10.1007/s10822-011-9432-2

Identification of novel inhibitors of mitogen-activated protein kinase phosphatase-1 with structure-based virtual screening

Hwangseo Park · Jeong-Yi Jeon · Song Yi Kim · Dae Gwin Jeong · Seong Eon Ryu

Received: 21 February 2011 / Accepted: 4 May 2011 / Published online: 13 May 2011

Abstract Mitogen-activated protein kinase phosphatase-1 (MKP-1) has proved to be an attractive target for the development of therapeutics for the treatment of cancer. We report the first example for a successful application of the structure-based virtual screening to identify the novel inhibitors of MKP-1. It is shown that the efficiency of virtual screening can be enhanced significantly by the incorporation of a new solvation energy term in the scoring function. The newly found inhibitors have desirable physicochemical properties as a drug candidate and reveal a moderate potency with IC_{50} values ranging from 20 to 50 μM. Therefore, they deserve a consideration for further development by structure–activity relationship studies to optimize the inhibitory activities. Structural features relevant to the stabilization of the inhibitors in the active site of MKP-1 are discussed in detail.

Keywords Virtual screening · Drug discovery · Docking · MKP-1 inhibitor · Solvation

H. Park (✉)
Department of Bioscience and Biotechnology, Sejong University, 98 Kunja-Dong, Kwangjin-Ku, Seoul 143-747, Korea
e-mail: hspark@sejong.ac.kr

J.-Y. Jeon · S. Y. Kim · S. E. Ryu
Department of Bioengineering, Hanyang University, 17 Haengdang-dong, Seongdong-gu, Seoul 133-791, Korea
e-mail: ryuse@hanyang.ac.kr

D. G. Jeong
Medical Proteomics Research Center, Korea Research Institute of Bioscience and Biotechnology, 52 Eoeun-Dong, Yuseong-Gu, Daejeon 305-333, Korea

Introduction

Mitogen-activated protein kinase phosphatase-1 (MKP-1) is a dual specificity phosphatase that hydrolyzes the phosphorylated threonine and tyrosine residues on a variety of mitogen-activated protein kinase (MAPK) substrates including p38, JNK, and ERKs. It has been considered to be involved in neoplasia, and therefore has drawn much interest as an attractive potential therapeutic target for cancer [1]. Indeed, the expression level of MKP-1 proved to be elevated in prostate, breast, gastric, and renal cancers [2, 3] with a strong correlation with the decrease in progression-free survival [4]. It was also demonstrated that the reduction in the expression level of MKP-1 would have an effect of restricting the possibility of tumorigenicity [5]. A series of experimental evidence have thus confirmed that MKP-1 should be a promising target for the discovery of anticancer drugs.

Nonetheless, the discovery of MKP-1 inhibitors has lagged behind the biochemical and pharmacological studies. Only a few structural classes of MKP-1 inhibitors have been reported so far. Several derivatives of benzofuran and benzo[*c*]phenanthridine alkaloid proved to be an effective inhibitors of MKP-1 with micromolar inhibitory activity [6, 7]. Recently, various adociaquinone B and naphthoquinone derivatives have also been identified as MKP-1 inhibitors with the additional inhibitory activities against MKP-3 and Cdc25 [8], which have also been considered to be a promising target for the development of anticancer drugs.

In the present study, we identify the novel classes of MKP-1 inhibitors by means of a structure-based drug design protocol involving the virtual screening with docking simulations and in vitro enzyme assay. Virtual screening with docking simulation has not always been successful due to the inaccuracy in the scoring function.

The characteristic feature that discriminates our virtual screening approach from the others lies in the implementation of an accurate solvation model in calculating the binding free energy between MKP-1 and the putative ligands, which would have an effect of increasing the hit rate in enzyme assay [9]. Indeed, the inclusion of the desolvation energy term in the scoring function can diminish the overestimation of the binding affinity of a ligand with many polar atoms. It will be shown that the docking simulations with the improved binding free energy function can be a useful tool for elucidating the activities of the identified inhibitors, as well as for enriching the chemical library with molecules that are likely to have desired biological activities.

Methods

Computational details

Although three dimensional (3D) structure of MKP-1 has not been reported so far, its structure can be predicted with homology modeling using the X-ray crystal structure of MKP-2 (PDB code: 3EZZ) [10] as the template. A high-quality 3D structure of MKP-1 is expected because the sequence identity between the two MKPs amounts to 86% [11], and they have the same amino acid sequence (C–Q–A-G-I–S) for the PTP loop (residues 258–264 for MKP-1) that is the key component of the active site. Homology modeling of MKP-1 with the X-ray structure of MKP-2 was carried out using the latest version of MODELLER program [12]. Ten structural models of MKP-1 were generated, and the one with the lowest value of MODELLER objective function was selected as the final model of MKP-1 to be used in the subsequent virtual screening with docking simulations.

A special attention was paid to assign the protonation states of the ionizable Asp, Glu, His, and Lys residues in the homology-modeled structure of MKP-1. The side chains of Asp and Glu residues were assumed to be neutral if one of their carboxylate oxygens pointed toward a hydrogen-bond accepting group including the backbone aminocarbonyl oxygen at a distance within 3.5 Å, a generally accepted distance limit for a hydrogen bond of moderate strength [13]. Similarly, the lysine side chains were assumed to be protonated unless the NZ atom was in proximity of a hydrogen-bond donating group. The same procedure was also applied to determine the protonation states of ND and NE atoms in His residues. Overall only one amino acid residue, Glu215, was found to have the unusual protonation state with the neutral carboxylic acid group in the side chain. Because Glu215 is ~20 Å distant from the active site, its protonation state seems to have little effect on the results of virtual screening.

The docking library for MKP-1 comprising about 240,000 compounds was constructed from the latest version of the chemical database distributed by Interbioscreen (http://www.ibscreen.com) containing approximately 477,000 synthetic and natural compounds. Prior to the virtual screening with docking simulations, they were filtrated on the basis of Lipinski's "Rule of Five" with the ISIS/BASE program to adopt only the compounds with the physicochemical properties of potential drug candidates [14] and without reactive functional group(s). To remove the structural redundancies in the docking library, the structurally similar compounds with Tanimoto coefficient larger than 0.8 were clustered into a single representative molecule. All of these pre-filtrated compounds were subjected to the CORINA program to generate their 3D atomic coordinates [15], followed by the assignment of Gasteiger-Marsilli atomic charges [16]. We used the AutoDock program of version 3.0.5 [17] in the virtual screening of MKP-1 inhibitors because the outperformance of its scoring function over those of the others had been shown in several target proteins [18]. AMBER force field parameters [19] were assigned to calculate van der Waals interactions and the internal energy of a ligand as implemented in the original AutoDock program. Docking simulations were then carried out in the active site of MKP-1 to score and rank the compounds in the docking library according to their calculated binding affinities.

In the actual docking simulation of the compounds, we used the empirical AutoDock scoring function improved by the implementation of a new solvation model for a compound. The modified scoring function has the following form:

$$\begin{aligned}\Delta G^{aq}_{bind} = {} & W_{vdW}\sum_{i=1}\sum_{j>i}\left(\frac{A_{ij}}{r_{ij}^{12}}-\frac{B_{ij}}{r_{ij}^{6}}\right) \\ & + W_{hbond}\sum_{i=1}\sum_{j>i}E(t)\left(\frac{C_{ij}}{r_{ij}^{12}}-\frac{D_{ij}}{r_{ij}^{10}}\right) \\ & + W_{elec}\sum_{i=1}\sum_{j>i}\frac{q_iq_j}{\varepsilon(r_{ij})r_{ij}} + W_{tor}N_{tor} \\ & + W_{sol}\sum_{i=1}S_i\left(Occ_i^{\max}-\sum_{j>i}V_je^{-\frac{r_{ij}^2}{2\sigma^2}}\right), \end{aligned} \quad (1)$$

where W_{vdW}, W_{hbond}, W_{elec}, W_{tor}, and W_{sol} are the weighting factors of van der Waals, hydrogen bond, electrostatic interactions, torsional term, and desolvation energy of the putative inhibitors, respectively. r_{ij} represents the interatomic distance, and A_{ij}, B_{ij}, C_{ij}, and D_{ij} are related to the depth of the potential energy well and the equilibrium separations between the protein and ligand atoms. The

hydrogen bond term has an additional weighting factor, $E(t)$, representing the angle-dependent directionality. A cubic equation approach was applied to obtain the dielectric constant, $\varepsilon(r_{ij})$, required in computing the interatomic electrostatic interactions between MKP-1 and a ligand molecule [20]. In the entropic term, N_{tor} is the number of all rotatable bonds in the ligand. In the desolvation term, S_i and V_i are the solvation parameter and the fragmental volume of atom i [21], respectively, while Occ_i^{max} stands for the maximum atomic occupancy. In the calculation of molecular solvation free energy term in Eq. 1, we used the atomic parameters developed in recent years by Kang et al. [22] because their solvation model proved to be successful in predicting the solvation free energies of a variety of organic molecules. This modification of the solvation free energy term is expected to increase the accuracy in virtual screening because the underestimation of ligand solvation often leads to the overestimation of the binding affinity of a ligand with many polar atoms [9].

Docking simulation of a compound in the docking library started with the calculation of the 3D grids of interaction energy for all possible atom types. These uniquely defined potential grids for MKP-1 were then used in common for docking simulations of all compounds in the library. As the center of the common grids in the active site, we used the center of mass coordinates of the docked structure of the probe molecule (sulfate ion) whose binding mode had been known in the active site of MKP-2 [10]. The calculated grid maps were of dimension 61 × 61 × 61 points with the spacing of 0.375 Å, yielding a receptor model that includes the atoms within 22.9 Å of the grid center. These grid maps are sufficient to cope with almost the entire part of the catalytic domain of MKP-1 including all amino acid residues in PTP, general acid, and E loops. For each compound in the library, 10 docking runs were performed with the initial population of 50 individuals. Maximum number of generations and energy evaluation were set to 27,000 and 2.5×10^5, respectively. The compounds with the lowest values of binding free energy were then selected as candidates for MKP-1 inhibitors.

In vitro enzyme assay

The catalytic domain of human MKP-1 (MKP-1c, residues 152–323) was subcloned into pET28a and overexpressed using *Escherichia coli* BL21 (DE3) strain. Cells were grown at 18 °C after induction with 0.1 mM IPTG for 16 h. His-tagged MKP-1c was purified by nickel-affinity chromatography and dialyzed against the buffer containing 20 mM Tris–HCl (pH 8.0), 0.2 M NaCl, and 5 mM DTT. 144 compounds selected from the precedent virtual screening were evaluated for their in vitro inhibitory activity against the recombinant MKP-1c. Assays were performed by monitoring the extent of hydrolysis of 6,8-difluoro-4-methyl-umbelliferyl phosphate (DiFMUP) with a spectrofluorometric assay. The purified MKP-1c (5 nM), DiFMUP (10 μM), and a candidate inhibitor were incubated in the reaction mixture containing 20 mM Tris–HCl (pH 8.0), 0.01% Trition X-100, and 5 mM DTT for 20 min. This enzymatic reaction was stopped with the addition of sodium orthovanadate (1 mM). The phosphatase activities were then checked by the absorbance changes due to the hydrolysis of the substrate at 460 nm. IC_{50} values of the inhibitors were determined from direct regression curve analysis in duplicate.

Results and discussion

The final structural model of MKP-1 obtained from homology modeling was evaluated with the ProSa 2003 program by examining whether the interaction of each residue with the remainder of the protein could be maintained favorable. This program calculates the knowledge-based mean fields to judge the quality of protein folds, and has been widely used to measure the stability of a protein conformation [23]. Figure 1 compares the ProSa 2003 energy profiles of the homology-modeled MKP-1 and the X-ray structure of MKP-2. We note that the ProSa energy remains negative for each amino acid residue in both cases, indicating that both of the protein structures should be acceptable. More interestingly, the homology-modeled structure of MKP-1 reveals the higher stability than the X-ray structure of MKP-2 in a large part of protein except for some N- and C-terminal residues, which demonstrates

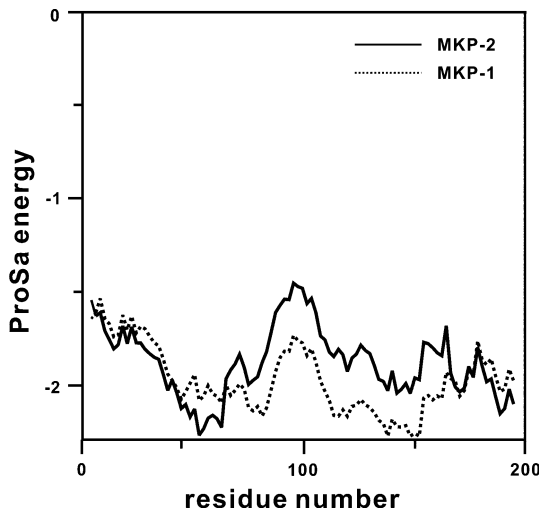

Fig. 1 Comparison of ProSa energy profiles for the homology-modeled structure of MKP-1 and the X-ray crystal structure of MKP-2. For convenience, the amino acids of both MKP phosphatases are renumbered from 1 instead of retaining their original numbers

the accuracy of the newly obtained structure of MKP-1. This result also supports the possibility that homology modeling using a template with a high sequence identity can produce a 3D structure of target protein comparable in accuracy to the X-ray crystal structure [12].

Of the 240,000 compounds subject to the virtual screening with docking simulations, 150 top-scored compounds were selected as virtual hits. 144 of them were available from the compound supplier and were tested for inhibitory activity against MKP-1 by in vitro enzyme assay. As a result, we identified four compounds that inhibited the catalytic activity of MKP-1 by more than 50% at the concentration of 50 μM, which were selected to determine the IC_{50} values. The chemical structures and the inhibitory activities of the newly identified inhibitors are shown in Fig. 2 and Table 1, respectively.

We note that compounds **1-4** share a carboxylate group at the end of the molecular structure. This carboxylate group seems to serve as a surrogate for the substrate phosphate group with the negative charge. The presence of a five-membered ring in the middle of the molecular structure is also a common feature among the four inhibitors. To the best of our knowledge, these compounds have not been reported as MKP inhibitors so far. Furthermore, no additional biological activity was found for the four inhibitors at least in the two most public chemical databases, ChEMBL and PubChem. As can be seen in Table 1, the four inhibitors reveal a moderate potency against MKP-1 with the IC_{50} values ranging from 20 to 50 μM. Therefore, they deserve a consideration for further development by structure–activity relationship (SAR) studies to optimize the inhibitory activities.

We addressed the energetic features associated with the binding of the inhibitors in the active site of MKP-1. Table 2 lists the calculated binding free energies of the four identified inhibitors. These four compounds were selected with the scoring function in which the desolvation term had been implemented. Keeping it in mind that the binding free energy of a protein–ligand complex in aqueous solution (ΔG_b^{aq}) can be approximated as the difference between that in the gas phase (ΔG_b^{gas}) and the solvation free energy of the ligand (ΔG^{sol}) [9], we computed the two energy components separately to estimate their relative contributions to ΔG_b^{aq}. It is noted that ΔG_b^{gas} values of **1** and **3** are higher than those of **2** and **4**. This indicates that the interactions of the inhibitors with the active site of MKP-1 get weaker with the introduction of a substituent at the nitrogen atom flanking the two carbonyl groups in the common imidazolidine-2,4-dione or thiazolidine-2,4-dione moieties. As a result, the rankings of **1** and **3** should be beyond 150 in the virtual screening with ΔG_b^{gas} only. This indicates that only **2** and **4** could be found in virtual screening with the previous scoring function, and all of the four inhibitors **1-4** could be identified as MKP-1 inhibitor only when the solvation term was included in the scoring function. Indeed, ΔG^{sol} becomes more negative in going from **1** and **3** to **2** and **4**, which implies that the former compounds should be less stabilized in aqueous solution than the latter ones. As a consequence of such a decrease in desolvation cost for the complexation of **1** and **3** in the active site of MKP-1, the magnitudes of their ΔG_b^{aq} values become comparable to those of **2** and **4**. **1** and **3** can thus be included in the hits of virtual screening in which the solvation energy term is taken into account, which exemplifies the superiority of the scoring function with the solvation

Table 1 Inhibitory activities of **1-4** against MKP-1

Compound	IC_{50} (μM)
1	23.4
2	24.9
3	37.7
4	44.4

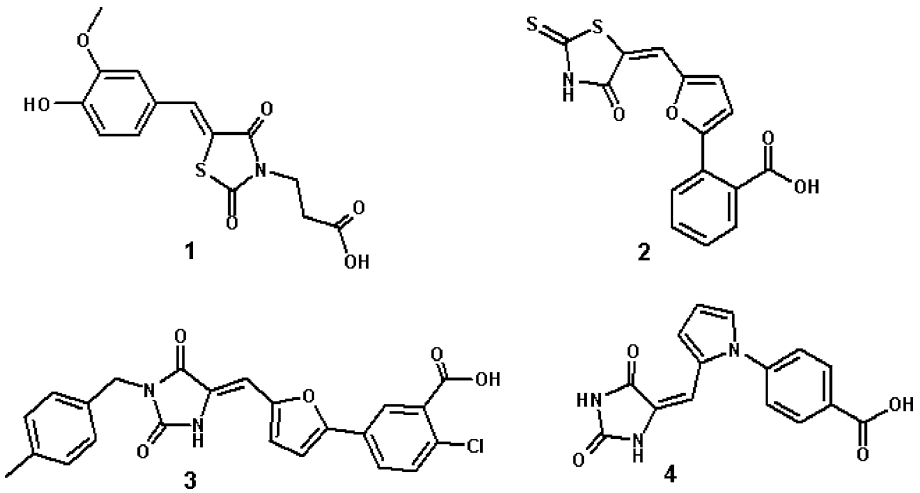

Fig. 2 Chemical structures of the newly identified MKP-1 inhibitors

Table 2 Calculated binding free energy in the gas phase, solvation free energy, and binding free energy in solution (kcal/mol) for the four MKP-1 inhibitors

Compound	ΔG_b^{gas}	ΔG^{sol}	ΔG_b^{aq}
1	−28.84 (152)	−6.06	−22.78 (25)
2	−30.25 (7)	−7.22	−23.03 (9)
3	−28.28 (197)	−5.87	−22.41 (38)
4	−29.81 (42)	−7.14	−22.67 (29)

Numbers in parenthesis indicate the rankings of the individual inhibitors in virtual screening

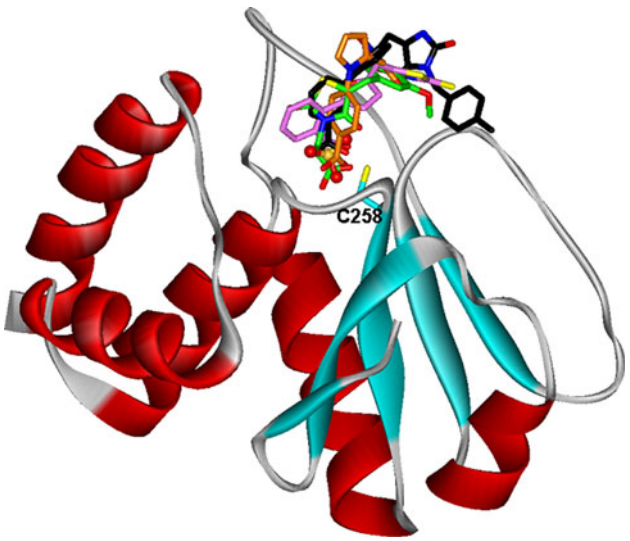

Fig. 3 Comparative view of the binding modes **1**-**4** in the active site of MKP-1. Carbon atoms of **1**, **2**, **3**, and **4** are indicated in *green*, *pink*, *black*, and *orange*, respectively. The substrate analogue (sulfate ion) is shown in *ball* and *stick*. The position of the catalytic residue Cys258 is also indicated. This figure was prepared with the ViewerPro program

term to the previous one. Such a large contribution of ΔG^{sol} to ΔG_b^{aq} also indicates that in order to enhance the potency of an inhibitor with a structural change, the resulting increase in the strength of enzyme-inhibitor interaction should be sufficient to surmount the increased stabilization in aqueous solution.

To obtain structural insight into the inhibitory mechanisms of the identified inhibitors of MKP-1, their binding modes in the active site were investigated in a comparative fashion. Figure 3 shows the lowest-energy conformations of **1-4** and the substrate analogue (sulfate ion) in active site gorge of MKP-1 calculated with the modified AutoDock program. The results of these docking simulations are self-consistent in the sense that the functional groups of similar chemical character are placed in similar ways with comparable interactions with the protein groups. As revealed by the superposition of their docked structures, for example, the carboxylate group of the inhibitors points toward the

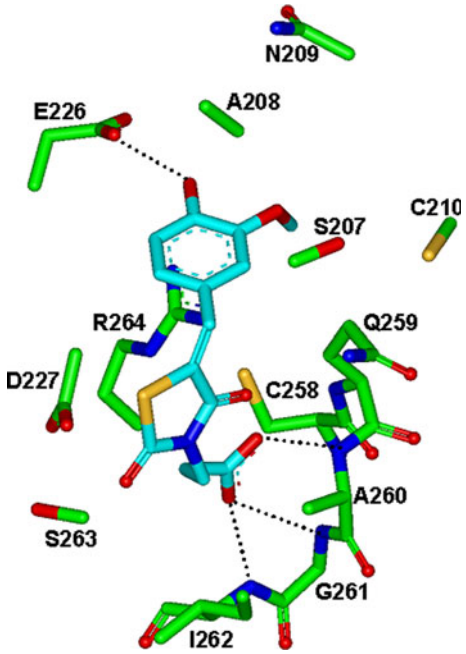

Fig. 4 Calculated binding mode of **1** in the active site of MKP-1. Carbon atoms of the protein and the ligand are indicated in *green* and *cyan*, respectively. Each *dotted line* indicates a hydrogen bond. This figure was prepared with the ViewerPro program

catalytic cystein residue (Cys258) with the hydrophobic groups residing between the two loop structures above the active site. The proximity of the inhibitor carboxylate group to Cys258 in all of the best-scored conformations indicates their necessity in the inhibition of MKP-1 as a surrogate for the substrate phosphate group. In order to examine the possibility of the allosteric inhibition of MKP-1 by the identified inhibitors, docking simulations were carried out with the grid maps for the receptor model so as to include the entire part of MKP-1. However, the binding configuration in which an inhibitor resides outside the active site was not observed for any of the new inhibitors. These results support the possibility that the inhibitors would impair the catalytic activity of MKP-1 through the specific binding in the active site.

We now turn to the identification of the detailed interactions responsible for the stabilization of each inhibitor in the active site. The calculated binding mode of **1** in the active site of MKP-1 is shown in Fig. 4. The inhibitor appears to be in a close contact with Cys258–Arg264, Glu226 and Asp227, and Ser207–Cys210, which belong to PTP, general acid, and E loops, respectively. It is noted that the carboxylate oxygens of the inhibitor receive three hydrogen bonds from the backbone amidic groups of Ala260, Gly261, and Ile262. This structural feature is consistent with that observed in the X-ray crystal structure of MKP-2 in complex with a substrate analogue of the sulfate group.[10] The formation of hydrogen bonds with the

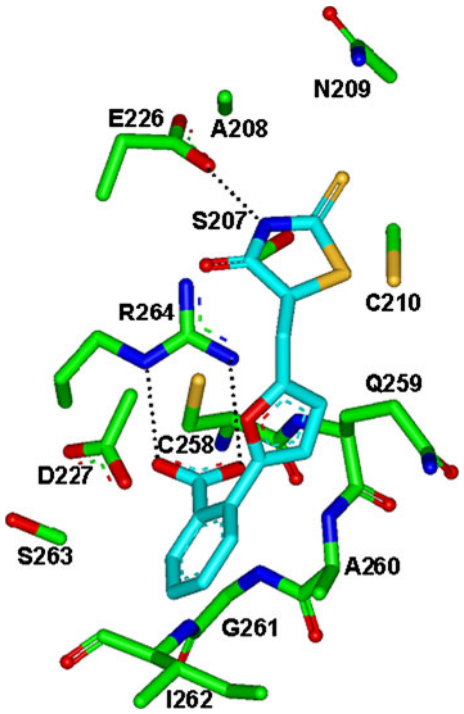

Fig. 5 Calculated binding mode of **2** in the active site of MKP-1. Carbon atoms of the protein and the ligand are indicated in *green* and *cyan*, respectively. Each *dotted line* indicates a hydrogen bond. This figure was prepared with the ViewerPro program

side-chain guanidium ion of Arg264 seems to be disfavored in MKP-1-**1** complex because of a large molecular length of **1** and the residence of Arg264 in the middle of the active site. Indeed, the binding configuration involving the hydrogen bond between the terminal carboxylate group of **1** and the side chain of Arg264 was not found despite the extensive docking simulations with varying parameters for calculating the binding modes. This indicates that **1** cannot be accommodated in the active site unless its terminal carboxylate group should be stabilized through the hydrogen bonds established at the bottom of the active site comprising the residues in the PTP loop. It is also noteworthy that the carbon atom of the inhibitor carboxylate group resides in the vicinity of the side-chain thiolate group of Cys258 with the associated interatomic distance of 3.51 Å. This distance is very similar to that between the sulfur atom of a substrate analogue and the catalytic residue of MKP-2 (3.53 Å) in the X-ray crystal structure. Judging from the proximity to Cys258 and the formation of the multiple hydrogen bonds in the active site, the carboxylate group seems to be an effective surrogate for the substrate phosphate group. A stable hydrogen bond is also established between the phenolic group of the inhibitor and the side-chain carboxylate group of Glu226. The formation of a hydrogen bond with Glu226 appears to be a common feature in the binding modes of the four inhibitors found in this study. The inhibitor **1** can be further stabilized in the active site by the hydrophobic interactions of its nonpolor groups with the side chains of Ala208, Ala260, and Ile262. Thus, the overall structural features derived from docking simulations indicate that the inhibitory activity of **1** stems from the multiple hydrogen bonds and hydrophobic interactions established simultaneously in the active site.

Figure 5 shows the lowest-energy binding mode of **2** in the active site of MKP-1. The binding mode of **2** differs from that of **1** in that the role of hydrogen bond donor for the inhibitor carboxylate moiety is played by the side-chain guanidium ion of Arg264 instead of the backbone amide groups at the bottom of the active site. As a seek for a binding configuration in which the carboxylate group is hydrogen-bonded to the backbone groups of the PTP loop, additional docking simulations were carried out in an extensive fashion with varying docking parameters. However, such a binding mode could not be found for **2**. This is not surprising because the negatively charged carboxylate group can be more stabilized by the positively charged guanidium ion than by the neutral amide groups. As in the MKP-1-**1** complex, however, the side-chain carboxylate group of Glu226 plays a role of hydrogen bond acceptor with respect to the aminocarbonyl nitrogen in the thiazolidine ring of **2** in the MKP-1-**2** complex. Hydrophobic interactions in the MKP-1-**2** complex are also established in a similar way to those in the MKP-1-**1** complex: its phenyl, furan, and thiazolidine rings form a van der Waals contact with the side chains of Ala208, Ala260, and Ile262. It is noteworthy that the number of hydrogen bonds decreases from four in the MKP-1-**1** to three in the MKP-1-**2** complex. However, the hydrogen bonds seem to be established in a stronger form in the latter than in the former because the positively charged guanidium group of Arg264 should be a better hydrogen bond donor than the neutral backbone amidic groups. The loss of one hydrogen bond can thus be compensated by establishing the stronger hydrogen bonds, which can be an explanation for the similar inhibitory activities of **1** and **2**. Binding modes of **3** and **4** appear to be similar to those of **1** and **2** in that the terminal carboxylate group and the aromatic rings are stabilized by the hydrogen bonds with the active-site residues and the hydrophobic interactions with nonpolar residues of MKP-1, respectively. Thus, it seems to be a common feature in binding modes of **1**–**4** that multiple hydrogen bonds and hydrophobic interactions contribute to the stabilization of the inhibitors in the active site in a cooperative fashion.

Conclusions

We have identified four novel inhibitors of MKP-1 by applying a computer-aided drug design protocol involving the structure-based virtual screening with docking

simulations under consideration of the effects of ligand solvation in the scoring function. These inhibitors have desirable physicochemical properties as a drug candidate and reveal a moderate potency with IC_{50} values ranging from 20 to 50 μM. Therefore, each of the newly discovered inhibitors deserves consideration for further development by SAR studies to optimize the inhibitory activities. Detailed binding mode analyses with docking simulations show that the inhibitors can be stabilized in active site by the simultaneous establishment of multiple hydrogen bonds and van der Waals contacts.

Acknowledgments This work was supported by Grant No. K11061 from the Korea Institute of Oriental Medicine (KIOM). A Hanyang University Internal Grant also supported this study.

References

1. Jeffery KL, Camps M, Rommel C, Mackay CR (2007) Targeting dual-specificity phosphatases: manipulating MAP kinase signalling and immune responses. Nat Rev Drug Discov 6:391–403
2. Magi-Galluzzi C, Mishra R, Fiorentino M, Montironi R, Yao H, Capodieci P, Wishnow K, Kaplan I, Stork PJ, Loda M (1997) Mitogen-activated protein kinase phosphatase 1 is overexpressed in prostate cancers and is inversely related to apoptosis. Lab Invest 76:37–51
3. Liao Q, Guo J, Kleeff J, Zimmermann A, Büchler MW, Korc M, Friess H (2003) Down-regulation of the dual-specificity phosphatase MKP-1 suppresses tumorigenicity of pancreatic cancer cells. Gastroenterology 124:1830–1845
4. Denkert C, Schmitt WD, Berger S, Reles A, Pest S, Siegert A, Lichtenegger W, Dietel M, Hauptmann S (2002) Expression of mitogen-activated protein kinase phosphatase-1 (MKP-1) in primary human ovarian carcinoma. Int J Cancer 102:507–513
5. Kikuchi K, Nakamura K, Shima H (1999) Protein phosphatases and cancer. Curr Top Biochem Res 1:75–87
6. Vogt A, Tamewitz A, Skoko J, Sikorski RP, Giuliano KA, Lazo JS (2005) The benzo[*c*]phenanthridine alkaloid, sanguinarine, is a selective, cell-active inhibitor of mitogen-activated protein kinase phosphatase-1. J Biol Chem 280:19078–19086
7. Lazo JS, Nunes R, Skoko JJ, de Oliveira PEQ, Vogt A, Wipf P (2006) Novel benzofuran inhibitors of human mitogen-activated protein kinase phosphatase-1. Bioorg Med Chem 14:5643–5650
8. Cao S, Murphy BT, Foster C, Lazo JS, Kingston DGI (2009) Bioactivities of simplified adociquinone B and naphthoquinone derivatives against Cdc25B, MKP-1, and MKP-3 phosphatases. Bioorg Med Chem 14:2276–2281
9. Shoichet BK, Leach AR, Kuntz ID (1999) Ligand solvation in molecular docking. Proteins 34:4–16
10. Jeong DG, Jung SK, Yoon TS, Woo EJ, Kim JH, Park BC, Ryu SE, Kim SJ (2009) Crystal structure of the catalytic domain of human MKP-2 reveals a 24-mer assembly. Proteins 76:763–767
11. Baker D, Sali A (2001) Protein structure prediction and structural genomics. Science 294:93–96
12. Sali A, Blundell TL (1993) Comparative protein modelling by satisfaction of spatial restraints. J Mol Biol 234:779–815
13. Jeffrey GA (1997) An introduction to hydrogen bonding. Oxford University Press, Oxford
14. Lipinski CA, Lombardo F, Dominy BW, Feeney PJ (1997) Experimental and computational approaches to estimate solubility and permeability in drug discovery and development settings. Adv Drug Deliver Rev 23:3–25
15. Gasteiger J, Rudolph C, Sadowski J (1990) Automatic generation of 3D atomic coordinates for organic molecules. Tetrahedron Comput Method 3:537–547
16. Gasteiger J, Marsili M (1980) Iterative partial equalization of orbital electronegativity-a rapid access to atomic charges. Tetrahedron 36:3219–3228
17. Morris GM, Goodsell DS, Halliday RS, Huey R, Hart WE, Belew RK, Olson AJ (1998) Automated docking using a Lamarckian genetic algorithm and an empirical binding free energy function. J Comput Chem 19:1639–1662
18. Park H, Lee J, Lee S (2006) Critical assessment of the automated AutoDock as a new docking tool for virtual screening. Proteins 65:549–554
19. Cornell WD, Cieplak P, Bayley CI, Gould R, Merz KM Jr, Ferguson DM, Spellmeyer DC, Fox T, Caldwell J, Kollman PA (1995) A second generation force field for the simulation of proteins, nucleic acids, and organic molecules. J Am Chem Soc 117:5179–5197
20. Park H, Jeon YH (2007) Cubic equation governing the outer-region dielectric constant of globular proteins. Phys Rev E 75:021916
21. Stouten PFW, Frömmel C, Nakamura H, Sander C (1993) An effective solvation term based on atomic occupancies for use in protein simulations. Mol Simul 10:97–120
22. Kang H, Choi H, Park H (2007) Prediction of molecular solvation free energy based on the optimization of atomic solvation parameters with genetic algorithm. J Chem Inf Model 47: 509–514
23. Sippl MJ (1993) Recognition of errors in three-dimensional structures of proteins. Proteins 17:355–362